Applied Surface Science 273 (2013) 661–669

Contents lists available at SciVerse ScienceDirect

Applied Surface Science

journal homepage: www.elsevier.com/locate/apsusc

CdS nanocrystals/TiO_2/crosslinked chitosan composite: Facile preparation, characterization and adsorption-photocatalytic properties

Huayue Zhu[a,b], Ru Jiang[b], Ling Xiao[a,*], Li Liu[a], Chunhua Cao[a], Guangming Zeng[c]

[a] Key Laboratory for Biomass-Resource Chemistry and Environmental Biotechnology of Hubei Province, Colledge of Resource and Environment Science, Wuhan University, Wuhan 430072, Hubei, PR China
[b] Laboratory of Resource Utilization and Pollution Control, College of Life Science, Taizhou University, Taizhou 318000, Zhejiang, PR China
[c] Key Laboratory of Environmental Biology and Pollution Control (Hunan University), Ministry of Education, Changsha 410082, Hunan, PR China

ARTICLE INFO

Article history:
Received 8 November 2012
Received in revised form 6 February 2013
Accepted 23 February 2013
Available online 4 March 2013

Keywords:
Adsorption
Photocatalysis
Azo dye
CdS
TiO_2

ABSTRACT

CdS nanocrystals deposited on TiO_2/crosslinked chitosan composite (CdS/TiO_2/CSC) were prepared in an attempt to photocatalyze decolorization of water soluble azo dye in aqueous solution under simulated solar light irradiation. CdS/TiO_2/CSC was characterized by X-ray diffraction (XRD), energy-dispersive spectroscopy (EDS), and scanning electron microscopy (SEM). The characterization results proved that CdS nanocrystals has successfully been deposited on/in TiO_2/crosslinked chitosan composite. The adsorption ability of CdS/TiO_2/CSC was approximately 2.66 mg methyl orange (a typical water soluble azo dye) per gram. The photocatalytic decolorization of methyl orange solution reached 99.1% by CdS/TiO_2/CSC after simulated solar light irradiation for 210 min. Kinetics analysis indicated that photocatalytic decolorization of methyl orange solution by CdS/TiO_2/CSC obeyed first-order kinetic Langmuir-Hinshelwood mechanism ($R^2 > 0.997$). CdS/TiO_2/CSC exhibited enhanced photocatalytic activity under simulated solar light irradiation compared with photocatalysts reported before and the photocatalytic activity of CdS/TiO_2/CSC maintained at 89.0% of initial decolorization rate after five batch reactions. The presence of NO_3^- accelerated the decolorization of methyl orange solution by CdS/TiO_2/CSC, while SO_4^{2-} and Cl^- had an inhibitory effect on the decolorization of methyl orange. Therefore, present experimental results indicated to assess the applicability of CdS/TiO_2/CSC as a suitable and promising photocatalyst for effective decolorization treatment of dye-containing effluents.

1. Introduction

In both developing and industrialized countries, a growing number of organic pollutants are discharged into all kinks of open waters [1]. Among those organic pollutants, soluble organic dyes are one of the major groups of pollutants in the wastewater. In China, over 1.6×10^9 m^3 of dye-containing wastewater per year is discharged into aquatic environment either directly or through the sewage treatment plants without proper treatment [2]. Dye-containing wastewater is characterized with high color, fluctuating pH, high chemical oxygen demand (COD), low biodegradability, and containing inorganic salts. The decolorization treatment of dye-containing wastewater is one of the most difficult issues to be solved because of its visibility and toxicity even at the very low concentration of soluble organic dyes. Therefore, great emphasis has been paid on the effective decolorization treatment of azo effluent by all kinds of methods [3,4].

Recently, heterogeneous photocatalysis based on semiconductor photocatalysts has attracted great attention as an environmentally friendly and cost-effective method for decolorization treatment of organic wastewater [5,6]. Among the semiconductors, nanosized titanium dioxide (TiO_2) is an excellent photocatalyst that can effectively degrade and mineralize all kinds of organic pollutants including soluble organic dyes [7]. However, the photocatalytic efficiency of raw TiO_2 so far is still low for practical application, mainly due to its wide band gap (3.2 eV) and high recombination rate of the photogenerated electron (e^-)–hole (h^+) pairs, which meant that only a small fraction of solar energy (3–5%) can be utilized [8]. In order to control the rate of recombination, the composition of two semiconductors with different band gaps can suppress the recombination of e^-/h^+ pairs, resulting in enhanced photocatalytic performance [9]. Recently, CdS/TiO_2 nanocomposite has shown much prospect as an effective visible light photocatalyst [7,10,11]. In the system of CdS/TiO_2, the photogenerated electrons in CdS are transferred into the TiO_2 particles while the holes remain

* Corresponding author at: Luojia Mountain of Wuchang, Wuhan City, Hubei Province 430072, PR China. Tel.: +86 139 7118 2725; fax: +86 027 68763162.
E-mail address: xiaoling9119@yahoo.cn (L. Xiao).

0169-4332/$ – see front matter © 2013 Elsevier B.V. All rights reserved.
http://dx.doi.org/10.1016/j.apsusc.2013.02.106

in the CdS particles [11]. However, the use of cadmium sulfide (CdS) as a photocatalyst has been limited due to its photocorrosion [10]. Recent researches indicated organic polymer films, such as chitosan films [12] or cellulose films [13,14], can ensure the stabilization of CdS nanoparticles and also provide an interface for the charge transfer, then correspondingly improve photocatalytic efficiency. In addition, chitosan can decrease the leakage of Cd(II) into the treated water during treatment since chitosan is an effective adsorbent and chelator for Cd(II) in aqueous solution [15,16].

In the present work, CdS nanocrystals deposited on TiO_2/crosslinked chitosan composite films (CdS/TiO_2/CSC in chief) were successfully prepared, in an attempt to photocatalyze decolorization of water soluble azo dyes (methyl orange as a model dye). The CdS/TiO_2/CSC was characterized by energy-dispersive spectroscopy (EDS), X-ray diffraction (XRD) and scanning electron microscopy (SEM). The photocatalytic activities of CdS/TiO_2/CSC under both simulated solar light irradiation and visible light irradiation were evaluated. The effects of inorganic anions, pH and reuse of photocatalyst on photocatalytic decolorization of methyl orange by CdS/TiO_2/CSC were examined. This information will be useful for further applications of CdS/TiO_2/CSC for the effective decolorization treatment of practical dye-containing effluents.

2. Experimental

2.1. Materials

Commercial anatase TiO_2 was purchased from Xiamen Micaren Technology Co., Ltd. (Xiamen, China), which was 10–25 nm in size and $210 \pm 10\ m^2\ g^{-1}$ in specific surface area. Chitosan with 92% of deacetylation degree was purchased from Yuhuan Ocean Biochemical Co., Ltd. (Taizhou, China). $CdCl_2$ and $(NH_2)_2CS$ were used to prepare CdS nanocrystals. Methyl orange (MO in chief, $C_{14}H_{14}O_3N_3SNa$, C.I.13025) as a model pollutant was obtained from Yongjia Fine Chemical Factory (Wenzhou, China). Other chemicals were of analytical grade from Shanghai Chemical Reagent Co., Ltd. (Shanghai, China). 0.1 mol L^{-1} NaOH or 0.1 mol L^{-1} HCl was used to adjust pH value of reaction solution. All reagents were used as received without further purification.

2.2. Preparation of CdS/TiO_2/CSC

Fig. 1 represents schematically the preparation of CdS/TiO_2/CSC by a simulating biomineralization method. Firstly, nanosized TiO_2 powder (0.3 g) and $CdCl_2$ (0.912 g) were mixed into 100 mL of 2% (w/v) chitosan acetate solution with ultrasonic stirring for 2 h. Subsequently, homogeneous suspension was cast evenly on clean glass plates. After drying under ambient temperature, thin gel films on glass plates were coagulated into 0.2 mol L^{-1} NaOH solution. Then, the solidified composite thin films were dipped into an equimolar amounts thiocarbamide aqueous solution in a water bath at 60 ± 0.2 °C in order to form nanosized CdS in the composite films slowly. To enhance water-resistant property, composite films were subsequently crosslinked by immersing into a 100 mL of 0.25% (v/v) glutaraldehyde solution for 30 min. Then the yellow composite thin films were washed using absolute ethanol and double distilled water for 3–4 time, respectively, in order to remove excess glutaraldehyde. Finally, the products (CdS/TiO_2/CSC in chief) were dried at 60 °C under atmospheric condition and cut into flakelets (about $1 \times 1\ mm^2$).

2.3. Characterization of CdS/TiO_2/CSC

XRD patterns were obtained using a Bruker D8 Advance X-ray diffractometer with Cu Kα radiation at a scanning rate of 6° 2θ min^{-1} in the 2θ range from 10° to 75°. The scanning electron microscopy (SEM) analysis was performed and energy-dispersive spectroscopy (EDS) was employed to determine the final actual element amounts with a Hitachi SX-650 scanning electron microscopy.

2.4. Adsorption of dye on CdS/TiO_2/CSC

For adsorption experiments, 50 mg of CdS/TiO_2/CSC was added into 100 mL of dye solution (15 mg L^{-1}). Samples were collected at different time intervals and the dye concentration (C_t) in the supernatant liquid was measured on a Varian UV-vis spectrophotometer (Cary 50, Varian Co. Ltd). The amount of dye adsorbed (q_t) onto the CdS/TiO_2/CSC was calculated as follows:

$$q_t = \frac{(C_0 - C_t)V}{m} \quad (1)$$

where C_0 and C_t are the initial and equilibrium solution concentrations (mg L^{-1}), respectively, V is the volume of the solutions (L) and m is the weight of CdS/TiO_2/CSC used (g).

2.5. Photocatalytic decolorization of MO dye

The photocatalytic activity of the as-prepared CdS/TiO_2/CSC was evaluated by photocatalytic decolorization of MO with a 300 W xenon lamp (PLS-SXE300, Beijing Trusttech Co., Ltd., China) as a light resource at 25 ± 0.5 °C. For visible light irradiation experiment, a UV cutoff filter ($\lambda > 400$ nm) only allowing the photons

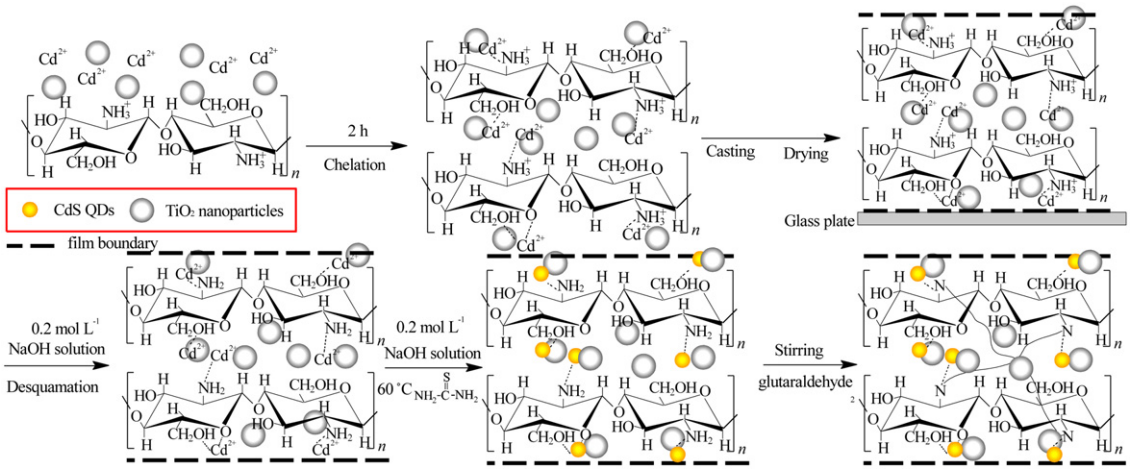

Fig. 1. The schematic mechanism for preparation of CdS/TiO_2/CSC.

with wavelengths above 400 nm to pass was used to provide visible light between the xenon lamp and the tube containing the reaction suspension. The distance between liquid surface of suspension and light source was set about 10 cm. The irradiation intensity was 68.8 mW cm^{-2} for simulated solar light source and 48.8 mW cm^{-2} for visible light source. In a typical run, 0.05 g of CdS/TiO_2/CSC was added to 100 mL of MO aqueous solution (15 mg L^{-1}). During photocatalytic decolorization, the resulting aqueous suspension containing MO and the photocatalyst was continuously stirred and bubbled so that the concentration of dissolved oxygen in reaction system was kept constant. Samples for analyses (about 4 mL) were taken and the filtrates were analyzed on a Varian UV-vis spectrophotometer (Cary 50, Varian Co. Ltd) at λ_{max} = 464 nm for MO solution. The effect of key operational factors, i.e. pH of solution, addition of coexisted anions, and reuse of photocatalyst on decolorization by CdS/TiO_2/CSC has been investigated systematically.

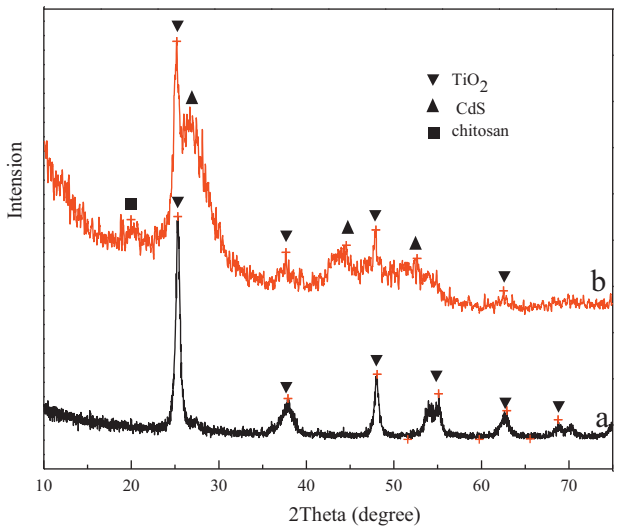

Fig. 2. XRD patterns of pure TiO_2 (a) and CdS/TiO_2/CSC (b).

3. Results and discussion

3.1. Characterization of CdS/TiO_2/CSC

Fig. 2 shows XRD patterns of TiO_2 and CdS/TiO_2/CSC. For the XRD pattern of TiO_2, the strongest peak at 2θ = 25.31°, 37.89°, 48.09°, 55.12°, 62.89° and 68.78 °clearly demonstrated the (1 0 1), (0 0 4), (2 0 0), (2 1 1), (2 0 4) and (1 1 6) anatase phase of TiO_2 nanocrystal, respectively(JCPDS 21-1272). The peak at 2θ = 20° in the XRD pattern of CdS/TiO_2/CSC was the typical characteristic angles for chitosan [17]. CdS/TiO_2/CSC displayed some obvious peaks at 2θ values of 25.20°, 37.66°, 47.93°, and 62.54°, assigned to anatase phase of TiO_2 nanocrystal. Meanwhile, the additional peaks at 26.93°, 44.56° and 52.65° were also observed in Fig. 2b, which were assigned to the CdS cubic phase (1 1 1), (2 2 0) and (3 1 1) crystal planes (JCPDS 89-0440). The average size of the nanocrystals structure of CdS in CdS/TiO_2/CSC calculated by analysis of XRD data of (1 1 1) was approximately 8 nm according to the Scherrer formula. However, the intensity of TiO_2 characteristic peaks in CdS/TiO_2/CSC weakened with the biosynthesis of CdS. As a result, cubic CdS nanocrystals and TiO2 anatase were co-existed in the samples in CdS/TiO_2/CSC.

Fig. 3 presents typical surface and cross-section SEM photographs and EDS of CdS/TiO_2/CSC. Obviously, many small particles

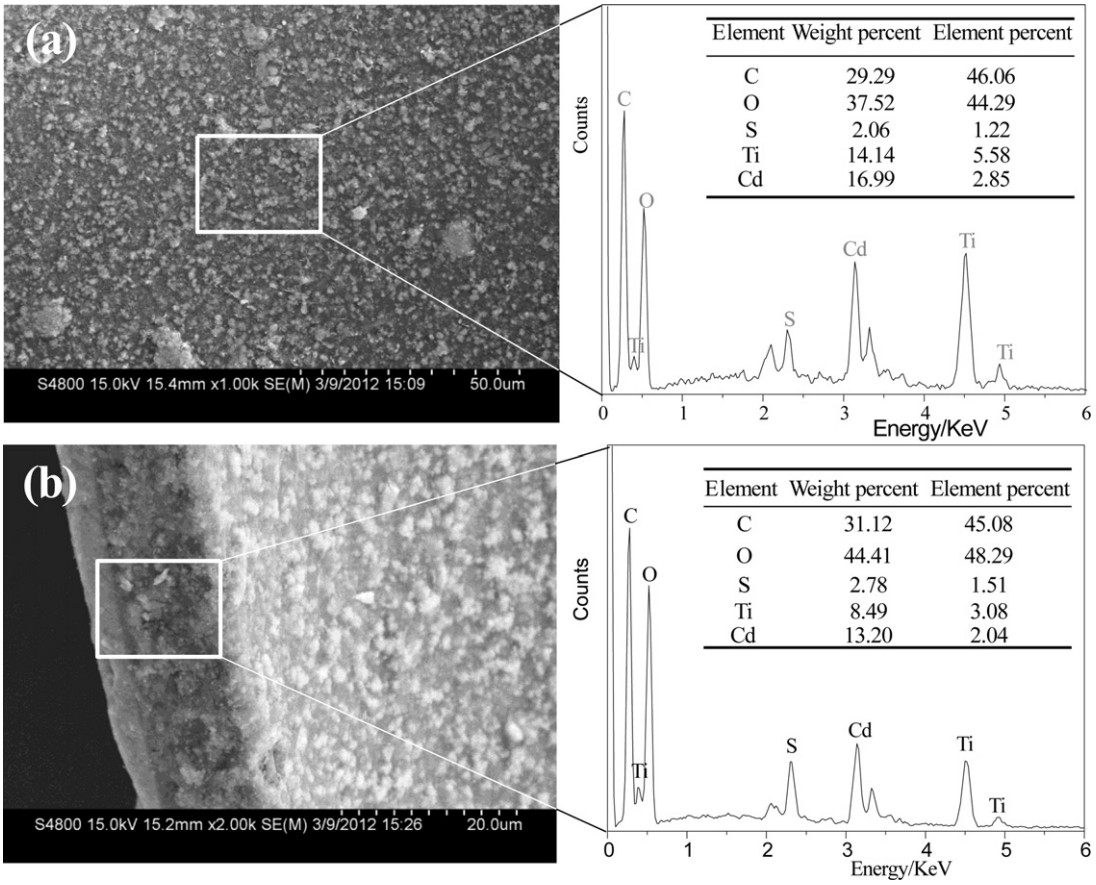

Fig. 3. SEM images and Energy dispersive spectra (EDS) of CdS/TiO_2/CSC: (a) the surface, (b) the cross-section.

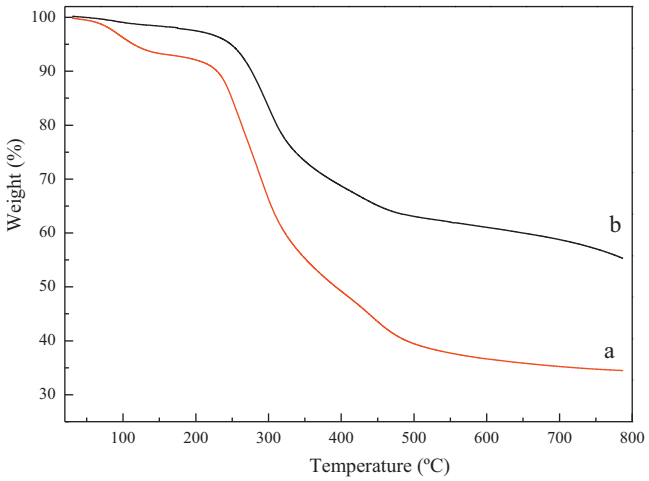

Fig. 4. TGA curves of chitosan films (a) and CdS/TiO_2/CSC (b).

had covered up the whole surface area and embedded in the cross-section area of CdS/TiO_2/CSC, which are speculated to be CdS and TiO_2 nanocrystal. Energy dispersive spectra (EDS) confirmed further that the CdS crystalline has deposited on nanosized TiO_2/crosslinked chitosan composite films. Both on the surface and in the cross-section, CdS/TiO_2/CSC composed with major elements such as C, O, Ti, Cd and S. The large amount of oxygen and carbon element resulted from chitosan matrix in CdS/TiO_2/CSC. In addition, the percent of CdS nanocrystals on the surface of CdS/TiO_2/CSC was higher than that in the cross-section, which made it high potential for decolorization of azo dye since photo-oxidation reaction usually took place at the surface of photocatalyst [18].

The thermal behaviors of chitosan films and CdS/TiO_2/CSC were investigated by TG analysis and the results were shown in Fig. 4. The TGA curve of chitosan films showed a typical polysaccharide behavior, which exhibited two distinct weight-loss stages. The first stage with weight loss of 8.8% was from room temperature to about 167 °C, which was related to the loss of water molecules adsorbed associated by hydrogen bonds. It is notable that the corresponding temperature was 167 °C, higher than in free water (usually 110 °C), which was maybe due to the strong hydrogen bonding between water molecule and the amino and hydroxyl groups of chitosan films [18]. The second stage with 53.6% of weight loss stared at about 217 °C and extended to 550 °C, which was caused by degradation of acetylated and deacetylated units of the polymer. The TGA curve of CdS/TiO_2/CSC also showed two stages of weight loss. However, the weight loss of CdS/TiO_2/CSC at fist stage was only 1.4% which was 7.4% less than that of the chitosan films, suggesting that the introduction of CdS and TiO_2 nanocrystals has deconstructed the hydrogen bonding between water molecule and the amino and hydroxyl groups of chitosan films. What's more, the total weight of the residue in CdS/TiO_2/CSC at 800 °C is 55.3%, which was 20.6% more than that of the chitosan films. The results supported that the CdS and TiO_2 nanocrystals has occupied almost in/on the chitosan matrix.

3.2. Adsorption behaviors of MO on CdS/TiO_2/CSC

Adsorption properties of photocatalyst towards pollutants are critical to photocatalytic reactions since it is well-known that the degraded substrates are firstly adsorbed onto the phtotocatalyst surface or free molecules arrive at the photocatalyst surface [19]. In order to investigate the adsorption behaviors of CdS/TiO_2/CSC towards MO molecules, dark adsorption experiments were carried out. 0.05 g of CdS/TiO_2/CSC was immersed directly in 100 mL MO solution with 15 mg L^{-1} for 5 h in dark. Adsorption kinetic models were applied to interpret the experimental data to determine the controlling mechanism of dye adsorption from aqueous solution on the photocatalyst.

The kinetics of adsorption of pollutants was investigated using Lagergren-first-order, pseudo-second-order and intra-particle diffusion reaction models [20–22]. The linear forms of Lagergren-first-order model, pseudo-second-order model and intra-particle mass transfer diffusion model are represented by Eq. (2)-(4), respectively.

$$\log(q_e - q_t) = \log q_e - \frac{k_1 t}{2.303} \quad (2)$$

$$\frac{t}{q_t} = \frac{1}{k_2 q_e^2} + \frac{1}{q_e} t \quad (3)$$

$$q_t = k_{id} t^{1/2} + c \quad (4)$$

where q_e and q_t are the amounts of MO adsorbed (mg g^{-1}) at equilibrium and at time t (min), respectively; k_1 is the rate constant of Lagergren-first-order kinetic model (min^{-1}); k_2 is the rate constant (g mg^{-1} min^{-1}) of pseudo-second-order kinetic model; c (mg g^{-1}) is the intercept and k_{id} is the intra-particle diffusion rate constant (mg g^{-1} $min^{-1/2}$). Values of k_1 can be calculated from the plots of log(q_e-q_t) versus t for Eq. (2). The slope and intercept of the linear plots of t/q_t against t yield the values of $1/q_e$ and $1/k_2 q_e^2$ for Eq. (3). According to Eq. (4), a plot of q_t versus $t^{1/2}$ could predict the sorption mechanism of the studied dye.

Three kinetic models for the adsorption of MO onto CdS/TiO_2/CSC are presented in Fig. 5. The kinetic parameters (k_1, k_2, k_{id}, q_e, c) and correlation coefficients (R^2) were calculated and are summarized in Table 1. The theoretical $q_{2e,cal}$ value estimated from pseudo-second-order kinetic model gave significantly different value compared with experimental values ($q_{e,exp}$), and the

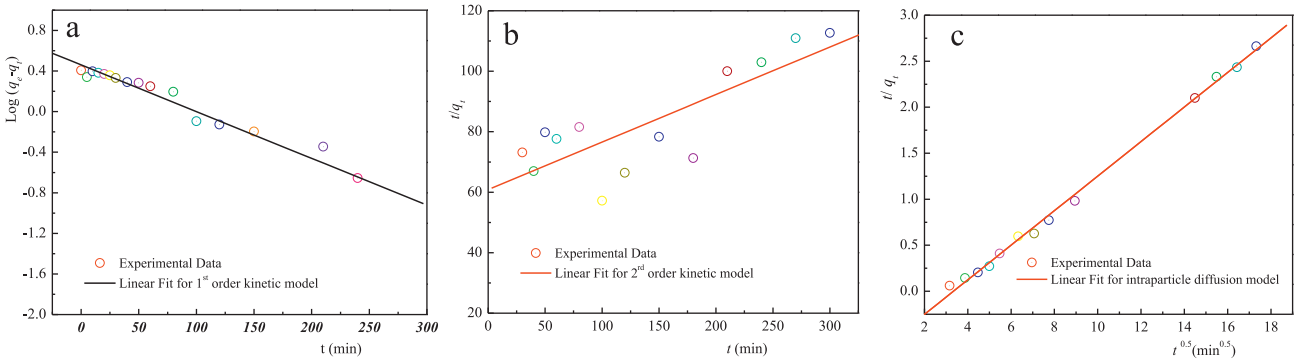

Fig. 5. Linear regressions of Lagergren-first-order model, pseudo-second-order kinetics and intra-particle diffusion models for adsorption of MO on CdS/TiO_2/CSC at 298 K (25 °C).

Table 1
Kinetic parameters of MO adsorption on CdS/TiO_2/CSC for 15 mg L^{-1} initial dye concentration.

Kinetic model	Kinetic parameters				
Lagergren-first-order kinetic model	$q_{e,exp}$(mg g^{-1})	$q_{1e,cal}$(mg g^{-1})	k_1(min^{-1})	R^2	SD (%)
	2.66	2.88	0.010594	0.966	0.077
Pseudo-second-order kinetic model	$q_{e,exp}$(mg g^{-1})	$q_{2e,cal}$(mg g^{-1})	k_2(g mg^{-1} min^{-1})	R^2	SD (%)
	2.66	6.36	0.000405	0.650	11.059
Intra-particle mass transfer diffusion model		k_i(mg g^{-1} $min^{-1/2}$)	c(mg g^{-1})	R^2	SD (%)
		0.1878	-0. 63	0.997	0.054

correlation coefficients (R^2 = 0.650) were also found to be lower. These results showed that the pseudo-second-order kinetic model didn't describe the MO adsorption on CdS/TiO_2/CSC. However, the values of the correlation coefficient (R^2) for the Lagergren-first-order kinetic model were ≥0.966 and the adsorption capacities calculated by the model ($q_{1e,cal}$) were also closer to that determined by experiments ($q_{e,exp}$). Therefore, it was feasible for the applicability of Lagergren -first-order kinetic model to describe the adsorption process of MO on CdS/TiO_2/CSC. In fact, Lagergren-first-order model has been widely used to define adsorption rates in some cases for the adsorption of dyes by chitosan [23] and chitosan/CNTs hydrogel beads [24].

The rate constant of intra-particle diffusion (k_{id}, mg g^{-1} $min^{-1/2}$), which is determined from the slope of the q_t versus $t^{0.5}$ plot, is utilized to determine the rate-determining step of the adsorption process. The linear plot obtained from the initial stage is shown in Fig. 5 c. The high correlation coefficient value (R^2 = 0.997 and SD = 0.054%) of the plot indicates that intra-particle diffusion might play a significant role in the initial stage of MO adsorption onto CdS/TiO_2/CSC. Generally, any adsorption processes take place through multi-step including the surface diffusion and the followed intra-particle diffusion [25]. The adsorption is governed by the liquid phase mass transport or by intra-particle mass transport. Since intra-particle diffusion mechanism was rate-determining step of the adsorption process, all model molecules can arrive immediately on the photocatalyst surfaces to be photocatalyze decolorization. Therefore, fast surface diffusion made it high potential for effective decolorization of azo dye since photo-oxidation reaction usually takes place on the surface of photocatalyst.

3.3. photocatalytic activities of CdS/TiO_2/CSC

To evaluate the photocatalytic activity of CdS/TiO_2/CSC, a series of experiments were carried out under the following different conditions: (a■) adsorption in dark; (b●) photocatalysis under visible light irradiation with a UV-cut filter; (c▲) photocatalysis under real solar light irradiation; (d▼) photocatalysis under simulated solar light irradiation. Initial concentration of MO dye was 15 mg L^{-1} and the amount of photocatalyst was 0.5 g L^{-1}. The corresponding results are shown in Fig. 6. 37.4% MO was photodecolorized by CdS/TiO_2/CSC under visible light in 300 min (Fig. 6 b), while only 8.9% of MO dye was adsorbed in dark (Fig. 6 a). Under simulated solar light irradiation, 99.1% color of MO solution was photocatalytic decolorized after 300 min (Fig. 6 d). There were some reasons for the remarkable docolorization by CdS/TiO_2/CSC under simulated solar light irradiation. At first, UV–vis absorption spectrum of CdS/TiO_2 in CdS/TiO_2/CSC could be shifted to approximately 550 nm, corresponding to band gap energy of 2.25 eV [11]. Secondly, UV light output (< 390 nm) of xenon lamp light resource was about 5.2% of irradiation energy while visible light output (390–770 nm) was about 39.2% according to a technical report on PLS-SXE300. Therefore, CdS/TiO_2/CSC could further be activated by UV light. What's more, the photogenerated electrons by CdS in CdS/TiO_2/CSC could be transferred into TiO_2 particles while the holes remain in the CdS particle under visible light irradiation [10]. In order to verify practical possibility of CdS/TiO_2/CSC under real solar light irradiation, photocatalytic experiments were also carried out on a sunny day of October from 10:00 a.m. to 15:00 p.m. The photocatalytic decolorization of MO reached 80.6% after real solar light irradiated for 300 min (Fig. 6c), which was 71.7% and 43.2% higher than in dark and under visible light irradiation, respectively.

The UV–vis spectra of MO solution in the presence of CdS/TiO_2/CSC at different light conditions are listed in Fig. 7. It can be seen from Fig. 7 that two major absorbance peaks can be seen at 270 and 464 nm in the initial UV–vis spectra of methyl orange, which are due to benzene ring and azo linkage [26]. During adsorption in dark, the absorbance at 464 nm decreased from 1.037 to 0.946 after 300 min while there is no shift of wavelength in MO solution (Fig. 7 a). However, these two absorbance peaks became weaker and weaker in intensity under three light irradiations as the irradiation time increased, accompanied by concomitant tiny hypsochromic shifts (Fig. 7b–d). Both the decrease in intensity and hypsochromic shifts of absorbance peaks are also meaningful with respect to the nitrogento-nitrogen double bond (—N=N—) of MO, as the most active site for oxidative attack [8,27]. Especially, after simulated solar light irradiation for 210 min, these two peaks of MO solution almost totally disappear, which indicates the benzene ring and azo linkage of most MO are destroyed by CdS/TiO_2/CSC. The results indicated that the prepared CdS/TiO_2/CSC can be used as a suitable and promising photocatalyst for effective decolorization treatment of dye-containing effluents.

3.4. Comparison of photocatalytic activity

To compare the photocatalytic activity of CdS/TiO_2/CSC with other photocatalysts, Langmuir–Hinshelwood (L-H) model was

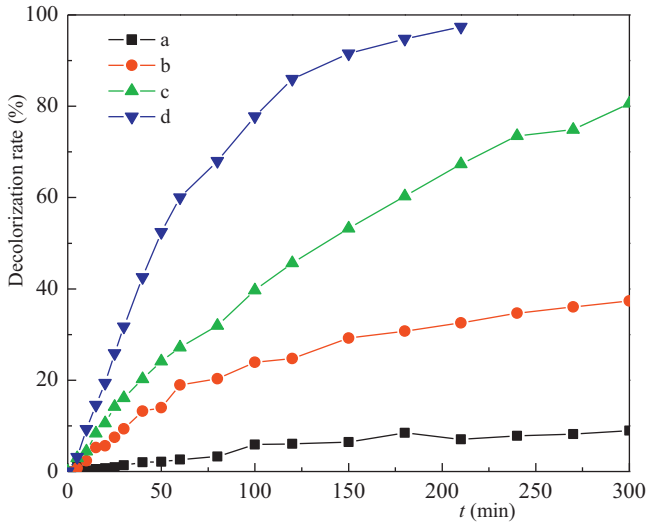

Fig. 6. Decolorization of MO by CdS/TiO_2/CSC under different experimental conditions. Light conditions: Adsorption in dark(a■); visible light irradiation with UV-cut filter (b●); real solar light irradiation(c▲); simulated solar light irradiation without UV-cut filter (d▼). Other experimental conditions: $[MO]_0$ = 15 mg L^{-1}; Photocatalyst dosage: 0.5 g L^{-1}; Air flow rate = 100 mL min^{-1}; pH = 5.6; T = 25 ± 1 °C.

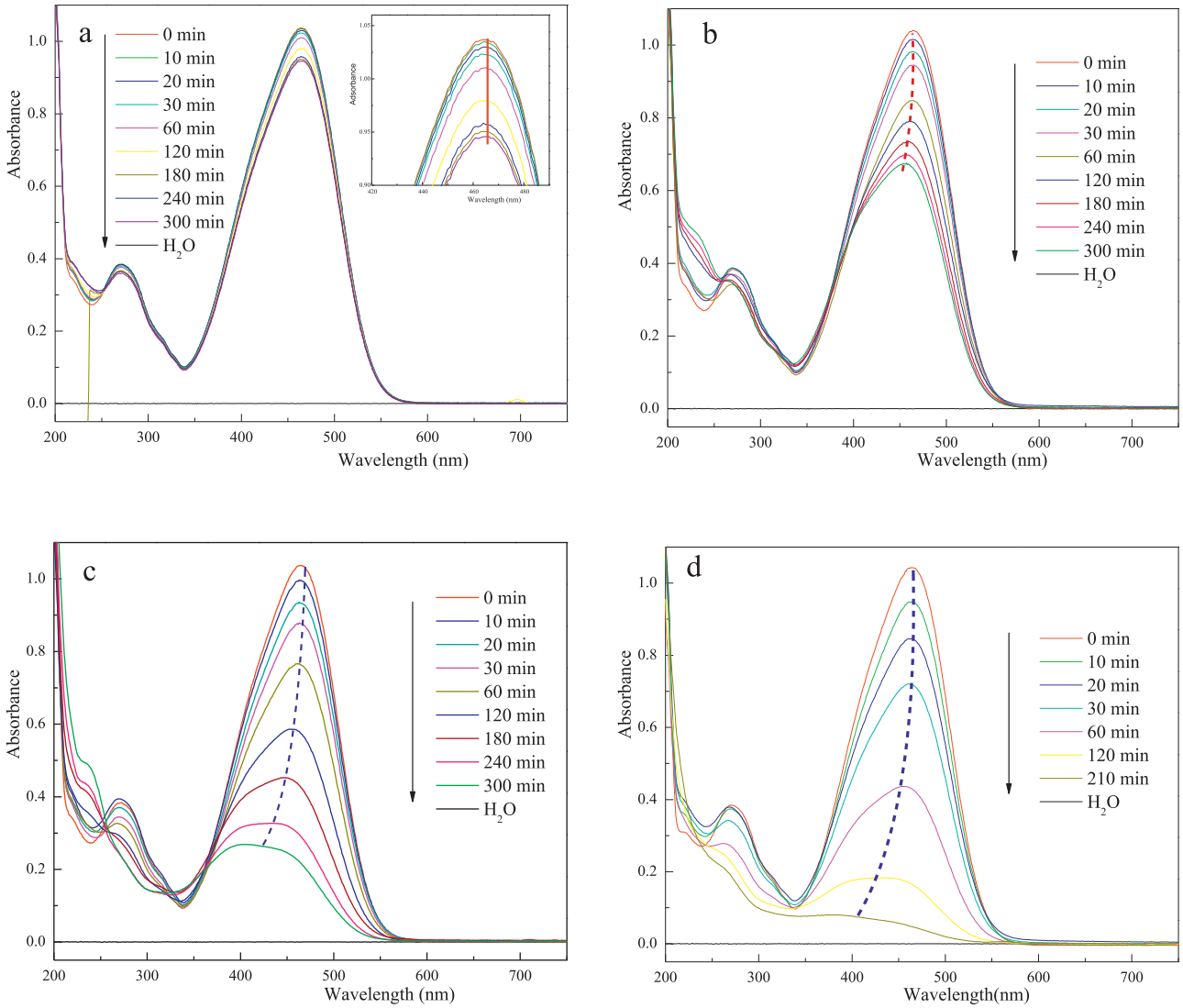

Fig. 7. Spectral change of MO solution by CdS/TiO_2/CSC at different light conditions. Light conditions: Adsorption in dark (a); visible light irradiation with UV-cut filter (b); real solar light irradiation(c); simulated solar light irradiation without UV-cut filter (d).

applied to calculate the corresponding photocatalytic rates of model pollutant [28]. When the initial concentration of pollutant is lower, Langmuir–Hinshelwood (L-H) model can be simplified to an apparent pseudo-first-order kinetics

$$ln\left(\frac{C_0}{C_i}\right) = k_{app}t \quad (5)$$

where k_{app} is the apparent pseudo-first-order reaction rate constant (min^{-1}). A plot of $ln(C_0/C_i)$ versus t will yield a slope of k_{app}. The value of k_{app} gives an indication for the photocatalytic activity of the photocatalyst.

The results are shown in Fig. 8. The high correlation coefficient ($R^2 > 0.997$) of linear regression indicated that photocatalytic decolorization of MO dye by CdS/TiO_2/CSC followed pseudo-first-order kinetic Langmuir–Hinshelwood mechanism. The values of k_{app} obtained directly from the linear regression analysis of the plots were 1.20×10^{-2} and 5.3×10^{-3} min^{-1} under real solar light irradiation and simulated solar light irradiation, respectively. The k_{app} values of MO photocatalytic decolorization on CdS/TiO_2/CSC have been compared with those of other photocatalysts reported by other researchers [29–31]. As shown in Table 2, the CdS/TiO_2/CSC had high photocatalytic activity and its photocatalytic efficiency under simulated solar irradiation (300 W xenon

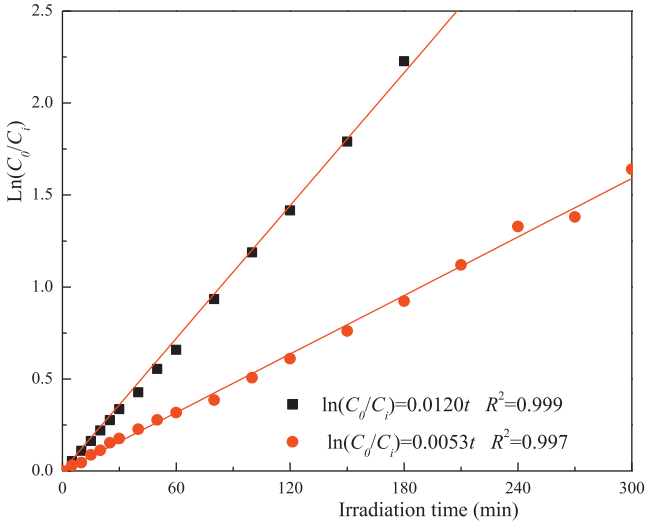

Fig. 8. Decolorization rate constants of MO by CdS/TiO_2/CSC under real solar light irradiation (●) and simulated solar light irradiation(■). Other experimental conditions: $[MO]_0$ = 15 mg L^{-1}; Photocatalyst dosage: 0.5 g L^{-1}; Air flow rate = 100 mL min^{-1}; pH = 5.6; T = 25 ± 1 °C.

Table 2
Comparison of photocatalytic kinetic parameters of MO solution by different photocatalysts.

Photocatalyst	k_{ap} (min^{-1})	Photocatalyst dosage (g^{-1})	Light type	C_0(mg L^{-1})	Ref.
CdS/TiO_2/CSC	1.20×10^{-2}	0.5	300 W xenon lamp	15	Present study
	5.3×10^{-3}	0.5	Real solar light	15	Present study
AgBr/TiO_2	8.00×10^{-3}	2.5	1000 Wxenon lamp	15	[31]
Pure ZnO nanorods	6.72×10^{-3}	/	365 nm irradiation	15	[30]
Pure ZnO film	2.19×10^{-5}	/	365 nm irradiation	15	[30]
TiO_2 powder	3.0×10^{-3}	0.5	UVA light	16	[29]

lamp) was higher than the AgBr/TiO_2 under simulated solar irradiation (1000 W xenon lamp) [31] pure ZnO nanorods and Pure ZnO film under 365 nm irradiation [30], TiO_2 powder under UVA light [29], revealing that CdS/TiO_2/CSC was suitable and promising material for the photocatalytic decolorization of dye pollutants from aqueous solutions since it displayed higher photocatalytic activity.

3.5. The reproducibility of CdS/TiO_2/CSC

In view of practical application, the photocatalyst should be chemically and optically stable after several repeated photocatalysis. To investigate the reusability of CdS/TiO_2/CSC in the photocatalytic reaction, the photocatalytic decolorization experiment was repeated five times. For each cycling run, the photocatalyst dosage, initial MO concentration, irradiation time and pH of MO solution were 0.5 g L^{-1}, 15 mg L^{-1}, 300 min and 5.6, respectively. After every decolorization experiment of MO solution, the resulting suspension was filtrated and CdS/TiO_2/CSC was recovered by washing with double distilled water and drying at 80 °C for 1 h. As shown in Fig. 9, after five times of cycle photocatalytic experiment, CdS/TiO_2/CSC did not show a clear decrease in photodecolorization efficiency. The decolorization percent decreased only from 98.4% to 87.6% after five cycles for CdS/TiO_2/CSC, which maintained at 89.0% of initial decolorization rate. Judging from these results, CdS/TiO_2/CSC was regarded to be relatively stable under the experimental condition and owned a better reproducibility of photocatalytic decolorization, which is possible to be used in practical process. Of course, further work is required to better understand factors that affect the decolorization rate of CdS/TiO_2/CSC and to improve further the photocatalyst stability.

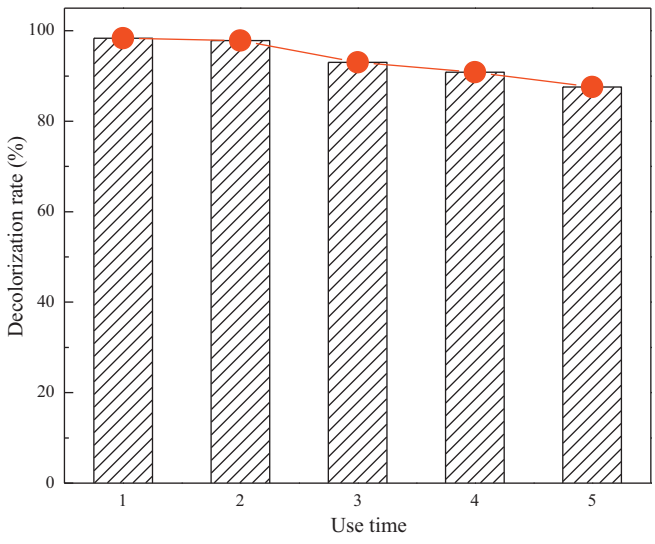

Fig. 9. Cycling runs of MO decolorization in the presence of CdS/TiO_2/CSC. Experimental conditions: $[MO]_0$ = 15 mgL^{-1}; Photocatalyst dosage: 0.5 g L^{-1}; Air flow rate = 100 mL min^{-1}; pH = 5.6; T = 25 ± 1 °C; Irradiation time:300 min).

3.6. Effect of solution pH on decolorization

Solution pH is one of dominant parameters controlling photocatalytic decolorizatoin of dye-containing wastewater by photocatalyst. Fig. 10 shows the photocatalytic decolorization of MO solution by CdS/TiO_2/CSC at three pH values. Obviously, increasing pH of dye solution could decrease the decolorization efficiency of MO solution by CdS/TiO_2/CSC. Nearly complete decolorization (99.7%) of MO solution was obtained under simulated solar light irradiation within 150 min at pH 2.0. However, 91.6% and 60.9% color of original MO within 150 min were decolorized when pH of solution increased to 6.0 and 12.0, respectively. High correlation coefficient values (R^2 > 0.996) indicated that the decolorization behavior still followed L–H model at different pH values. However, the photocatalytic decolorization rate of MO by CdS/TiO_2/CSC at pH 2.0 is about 4.75 times higher than that at pH 12.0. Similar effect trend of pH were previously observed for the photodecolorization of MO solution by other photocatalyst [26,32]. Firstly, pH changes can influence the adsorption of dye molecules onto the photocatalyst surfaces, an important step for the photocatalytic oxidation to take place [19,33]. Chitosan has primary amino groups with pK_a value close to 6.5 [34]. The point of zero charge of the TiO_2 (Degussa P25) is at pH 6.25; the surface of TiO_2 is positively charged at pH values less than 6.25 [35]. As a result, the surface of CdS/TiO_2/CSC is positively charged at pH values less than 6.5. However, the pKa of MO is generally reported at pH about 3.46. Therefore, a strong adsorption of MO dye on the CdS/TiO_2/CSC took place in acid solution as a result of the electrostatic attraction of the positively charged CdS/TiO_2/CSC with the MO anions. It is common that the oxidation attack of the hole is the rate determining step at low pH, then this will lead to an increasing photocatalytic decolorization [36]. In addition, the structure of MO is the azo structure at higher pH, which was difficult to break by photocatalytic process [9].

3.7. Effect of electrolytes on decolorization

In practical dyes effluent, various electrolytes (such as NO_3^-, Cl^- and SO_4^{2-}) are often added into dyeing bath in textile industries in order to retard dyeing rate or improve color fastness [37,38]. Therefore, the existence of inorganic anions such as chloride (Cl^-), nitrate (NO_3^-) and sulfate (SO_4^{2-}) is considerably common in wastewater, especially in practical textile industry effluents. Therefore, the effects of co-existed anions on photocatalytic decolorization and degradation of dyes wastewater cannot be neglected. In this study, the effect of inorganic anions on the photocatalytic decolorization of MO by CdS/TiO_2/CSC under simulated solar light irradiation was studied by adding corresponding salts into the reaction solution at concentrations of 0.01 M and the corresponding results are shown in Fig. 11. In the absence of added anions 91.6% MO was decolorized within 150 min of simulated solar light irradiation whereas in the presence of sulfate, chloride and nitrate 76.8%, 85.6% and 96.6% MO solution was decolorized over the same period, respectively. Obviously, the presence of NO_3^- accelerated the decolorization of MO by CdS/TiO_2/CSC, while SO_4^{2-} and Cl^- had an inhibitory effect on the decolorization of MO. Chang and Kuo [39] also reported that

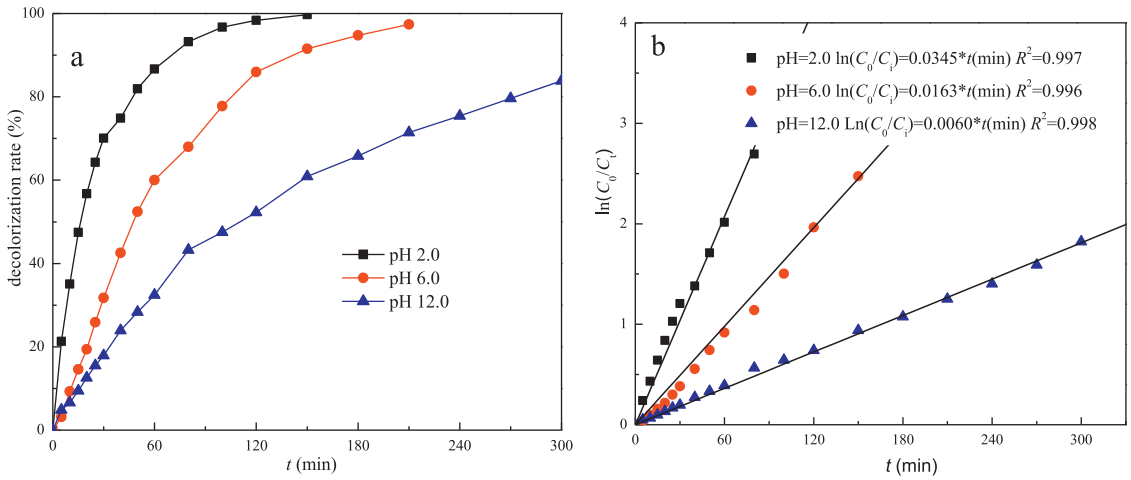

Fig. 10. Effect of solution pH value on the photocatalytic degradation of MO. Experimental conditions: $[MO]_0 = 15\ mg\ L^{-1}$; Photocatalyst dosage: $0.5\ g\ L^{-1}$; Air flow rate = 100 mL min^{-1}; T = 25 ± 1 °C.

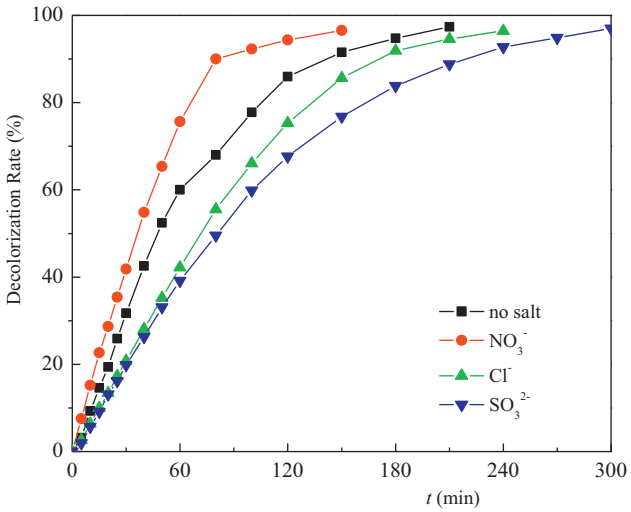

Fig. 11. Effect of different inorganic ions on the photocatalytic degradation of MO. Experimental conditions: $[MO]_0 = 15\ mg\ L^{-1}$; [Anion] = 0.01 M; Photocatalyst dosage: $0.5\ g\ L^{-1}$; Air flow rate = 100 mL min^{-1}; pH = 5.6; T = 25 ± 1 °C.

the presence of $NaNO_3$ had positive effect on the photodegradation of same dye. The enhancement of decolorization rate by NO_3^- may be resulted from the direct or indirect formation of hydroxyl radical [40]. At lower anion concentrations, Cl^- and SO_4^{2-} ions competed for oxidizing radicals or active sites of the photocatalyst, resulting in some degree of scavenging effects [41,42]. Though the presence of examined anions has influence on photocatalytic decolorization of MO solution by CdS/TiO_2/CSC, 90–95% color removal was still achieved in 300 min under simulated solar light irradiation whether anionic species present or not.

4. Conclusions

The characterization results suggested that CdS nanocrystalss have been deposited on TiO_2/crosslinked chitosan composite by a simulating biomineralization method. The photocatalytic decolorization of methyl orange solution reached 99.1% after real solar light irradiated for 300 min, which was 71.7% and 43.2% higher than those in dark and under visible light irradiation, respectively. Kinetics analysis indicated that photocatalytic decolorization of MO solution by CdS/TiO_2/CSC obeyed first-order kinetic Langmuir–Hinshelwood mechanism ($R^2 > 0.997$). The CdS/TiO_2/CSC exhibited enhanced photocatalytic activity under the simulated solar light irradiation compared with reported photocatalysts. The CdS/TiO_2/CSC could be used repeatedly and the photocatalytic activity of the photocatalyst was found to maintain at 89.0% of initial decolorization rate after five batch reactions. The presence of NO_3^- accelerated evidently the degradation of MO by CdS/TiO_2/CSC, while SO_4^{2-} and Cl^- had an inhibitory effect on the decolorization of MO. The prepared CdS/TiO_2/CSC may be promising photocatalytic material for decolorization treatment of dye-containing effluents.

Acknowledgements

This research was supported by the Natural Science Foundation of China (Grant No. 21007044 and 51208331) and the Domestic Visitor Foundation for Outstanding Young Teachers in the Higher Education Institutions from the Education Ministry of China.

References

[1] M.A. Shannon, P.W. Bohn, M. Elimelech, J.G. Georgiadis, B.J. Mariñas, A.M. Mayes, Science and technology for water purification in the coming decades, Nature 452 (2008) 301–310.
[2] J. Hu, Z. Song, L. Chen, H. Yang, J. Li, R. Richards, Adsorption properties of MgO(111) nanoplates for the dye pollutants from wastewater, Journal of Chemical and Engineering Data 55 (2010) 3742–3748.
[3] L.C. Ling, N. Morad, T.T. Teng, N. Ismail, Treatment of terasil red R dye wastewater using H_2O_2/pyridine/Cu(II) system, Journal of Hazardous Materials 168 (2009) 383–389.
[4] H.Y. Zhu, Y.Q. Fu, R. Jiang, J. Yao, L. Xiao, G.M. Zeng, Novel magnetic chitosan/poly (vinyl alcohol) hydrogel beads: preparation, characterization and application for adsorption of dye from aqueous solution, Bioresource Technology 105 (2012) 24–30.
[5] W. Du, Q. Sun, X. Lv, Y. Xu, Enhanced activity of iron oxide dispersed on bentonite for the catalytic degradation of organic dye under visible light, Catalysis Communications 10 (2009) 1854–1858.
[6] H.Y. Zhu, L. Xiao, R. Jiang, G.M. Zeng, L. Liu, Efficient decolorization of azo dye solution by visible light–induced photocatalytic process using SnO_2/ZnO heterojunction immobilized in chitosan matrix, Chemical Engineering Journal 172 (2011) 746–753.
[7] U.G. Akpan, B.H. Hameed, Parameters affecting the photocatalytic degradation of dyes using TiO_2-based photocatalysts: a review, Journal of Hazardous Materials 170 (2009) 520–529.
[8] M.A. Behnajady, N. Modirshahla, H. Fathi, Kinetics of decolorization of an azo dye in UV alone and UV/H_2O_2 processes, Journal of Hazardous Materials B136 (2006) 816–821.
[9] H.Y. Zhu, R. Jiang, Y.Q. Fu, Y.J. Guan, J. Yao, L. Xiao, G.M. Zeng, Effective photocatalytic decolorization of methyl orange utilizing TiO_2/ZnO/chitosan nanocomposite films under simulated solar irradiation, Desalination 286 (2012) 41–48.
[10] Y. Bessekhouad, N. Chaoui, M. Trzpit, N. Ghazzal, D. Robert, J.V. Weber, UV–vis versus visible degradation of Acid Orange II in a coupled CdS/TiO_2

semiconductors suspension, Journal of Photochemistry and Photobiology A 183 (2006) 218–224.
[11] L. Wu, J.C. Yu, X. Fu, Characterization and photocatalytic mechanism of nanosized CdS coupled TiO_2 nanocrystals under visible light irradiation, Journal of Molecular Catalysis A 244 (2006) 25–32.
[12] R. Jiang, H.Y. Zhu, J. Yao, Y.Q. Fu, Y.J. Guan, Chitosan hydrogel films as a template for mild synthesis of CdS quantum dots with highly efficient photocatalytic activity, Applied Surface Science 258 (2012) 3513–3518.
[13] D. Ke, S. Liu, K. Dai, J. Zhou, L. Zhang, T. Peng, CdS/regenerated cellulose nanocomposite films for highly efficient photocatalytic H_2 production under visible light irradiation, Journal of Physical Chemistry C 113 (2009) 16021–16026.
[14] J. Yang, J. Yu, J. Fan, D. Sun, W. Tang, X. Yang, Biotemplated preparation of CdS nanoparticles/bacterial cellulose hybrid nanofibers for photocatalysis application, Journal of Hazardous Materials 189 (2012) 377–383.
[15] A.K. Mishra, A.K. Sharma1, Synthesis of γ-cyclodextrin/chitosan composites for the efficient removal of Cd(II) from aqueous solution, International Journal of Biological Macromolecules 49 (2011) 504–512.
[16] M. Monier, D.A. Abdel–Latif, Preparation of cross-linked magnetic chitosan–phenylthiourea resin for adsorption of Hg(II), Cd(II) and Zn(II) ions from aqueous solutions, Journal of Hazardous Materials 209-210 (2012) 240–249.
[17] S. Lu, X. Song, D. Cao, Y. Chen, K. Yao, Preparation of water-soluble chitosan, Journal of Applied Polymer Science 91 (2004) 3497–3503.
[18] M.S.P. De Lima, M.S. Freire, J.L.C. Fonseca, M.R. Pereira, Chitosan membranes modified by contact with poly(acrylic acid), Carbohydrate Research 344 (2009) 1709–1715.
[19] C. Tang, V. Chen, The photocatalytic degradation of reactive black 5 using TiO_2/UV in an annular photoreactor, Water Research 38 (2004) 2775–2781.
[20] Y.S. Ho, Second-order kinetic model for the sorption of cadmium onto tree fern: a comparison of linear and non–linear methods, Water Research 40 (2006) 19–125.
[21] S. Lagergren, Zur theorie der sogenannten adsorption geloter stoffe, Kungliga Svenska Vetenskapsakademiens Handlingar 24 (1898) 1–39.
[22] J. Weber, W.J.J.C. Morris, Morris, Kinetics of adsorption on carbon from solution, Journal of Sanitary Engineering Division ASCE 89 (SA2) (1963) 31–59.
[23] Y.C. Wong, Y.S. Szeto, W.H. Cheung, G. McKay, Pseudo-first-order kinetic studies of the sorption of acid dyes onto chitosan and chitosan/CNTs beads, Journal of Applied Polymer Science 92 (2004) 1633–1645.
[24] C. Sudipta, M.W. Lee, S.H. Woo, Adsorption of congo red by chitosan hydrogel beads impregnated with carbon nanotubes, Bioresource Technology 101 (2010) 1800–1806.
[25] W. Plazinski, W. Rudzinski, A. Plazinsk, Theoretical models of sorption kinetics including a surface reaction mechanism: A review, Advances in Colloids and Interface Science 152 (2009) 2–13.
[26] S. Al–Qaradawi, S.R. Salman, Photocatalytic degradation of methyl orange as a model compound, Journal of Photochemistry and Photobiology A 148 (2002) 161–168.
[27] N.M. Mahmoodi, M. Arami, N.Y. Limaee, N.S. Tabrizi, Decolorization and aromatic ring degradation kinetics of Direct Red 80 by UV oxidation in the presence of hydrogen peroxide utilizing TiO_2 as a photocatalyst, Chemical Engineering Journal 112 (2005) 191–196.
[28] N. Daneshvar, M.H. Rasoulifard, A.R. Khataee, F. Hosseinzadeh, Removal of C.I. Acid Orange 7 from aqueous solution by UV irradiation in the presence of ZnO nanopowder, Journal of Hazardous Materials 143 (2007) 95–101.
[29] A. Luminita, D. Anca, The influence of TiO_2 powder and film on the photodegradation of methyl orange, Materials Chemistry and Physics 112 (2008) 1078–1082.
[30] J.J. Wu, C.H. Tseng, Photocatalytic properties of nc-Au/ZnO nanorod composites, Applied Catalysis B 66 (2006) (2006) 51–57.
[31] Y.J. Zang, R. Farnood, Photocatalytic activity of AgBr/TiO_2 in water under simulated sunlight irradiation, Applied Catalysis B 79 (2008) 334–340.
[32] M. Huang, C. Xu, Z. Wu, Y. Huang, J. Lin, J. Wu, Photocatalytic discolorization of methyl orange solution by Pt modified TiO_2 loaded on natural zeolite, Dyes Pigments 77 (2008) 327–334.
[33] S. Tunesi, M. Anderson, Influence of chemisorption on the photodecomposition of salicylic acid and related compounds using suspended titania ceramicmembranes, Journal of Physical Chemistry 95 (1991) 3399–3405.
[34] W. Liu, S. Sun, Z. Cao, X. Zhang, K. Yao, W.W. Lu, K.D.K. Luk, An investigation on the physicochemical properties of chitosan/DNA polyelectrolyte complexes, Biomaterials 26 (2005) 2705–2711.
[35] M. Saquiba, M.A. Tariqa, M.M. Haquea, M. Muneer, Photocatalytic degradation of disperse blue 1 using UV/TiO2/H2O2 process, Journal of Environment Management 88 (2008) (2008) 300–306.
[36] D. Bahnemann, D. Bockelmann, R. Goslich, Mechanistic studies of water detoxification in illuminated TiO_2 suspensions, Solar Energy Materials 24 (1991) 564–583.
[37] R. Jiang, Y.J. Guan, H.Y. Zhu, Y.Q. Fu, Effect of inorganic anions on photocatalytic decolorization of aqueous azo dye by CdS/polymer nanocomposite films under visible light irradiation, Coloration Technology 127 (2011) 426–433.
[38] A. Riga, K. Soutsas, K. Ntampegliotis, V. Karayannis, G. Papapolymerou, Effect of system parameters and of inorganic salts on the decolorization and degradation of Procion H-exl dyes. Comparison of H_2O_2/UV, Fenton, UV/Fenton, TiO_2/UV and TiO_2/UV/H_2O_2 processes, Desalination 211 (2007) 72–86.
[39] J.S. Chang, T.S. Kuo, Kinetics of bacterial decolorization of azo dye with *Escherichia coli* NO_3, Bioresource Technology 75 (2010) 107–111.
[40] M.A. Malouki, B. Lavédrine, C. Richard, Phototransformation of methabenthiazuron in the presence of nitrate and nitrite ions, Chemosphere 60 (2005) 1523–1529.
[41] W. Zhang, T. An, M. Cui, G. Sheng, J. Fu, Effects of anions on the photocatalytic and photoelectrocatalytic degradation of reactive dye in a packed-bed reactor, Journal of Chemical Technology and Biotechnology 80 (2005) 223–229.
[42] C. Hu, J.C. Yu, Z. Hao, P.K. Wong, Effects of acidity and inorganic ions on the photocatalytic degradation of different azo dyes, Applied Catalysis B 46 (2003) 35–47.